

Carboxylation of a μ_3 -Diazo Methylidyne Triosmium Cluster

S. M. Tareque Abedin,[†] Kenneth I. Hardcastle,[‡] Shariff E. Kabir,[†]
K. M. Abdul Malik,[§] M. Abdul Mottalib,[†] Edward Rosenberg,^{*,‡} and
M. Joynal Abedin[‡]

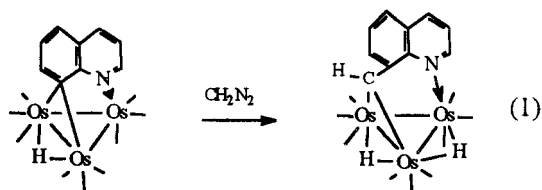
Department of Chemistry, Jahangirnagar University, Savar, Dhaka-1342, Bangladesh,
Department of Chemistry, Emory University, Atlanta, Georgia, Department of Chemistry,
University of Wales Cardiff, P.O. Box 912, Park Place,
Cardiff CF1 3TB, U.K., and Department of Chemistry, The University of Montana,
Missoula, Montana 59812

Received April 18, 2000

The unsaturated cluster $\text{Os}_3(\text{CO})_8(\text{Ph}_2\text{PCH}_2\text{P}(\text{Ph})\text{C}_6\text{H}_4)(\mu\text{-H})$ (**1**) reacts with CH_2N_2 at -10 to 25°C to give two novel compounds $\text{Os}_3(\text{CO})_7(\mu_3\text{-CN}_2)(\mu\text{-dppm})(\mu\text{-H})_2$ (**2**) and $\text{Os}_3(\text{CO})_7(\mu_3\text{-CCO}_2\text{H})(\mu\text{-dppm})(\mu\text{-H})_3$ (**3**) characterized by single-crystal X-ray crystallography. Compound **2** is converted to **3** in almost quantitative yield by reaction with CO (atmospheric pressure) and trace H_2O . The reaction of **2** with molecular hydrogen at atmospheric pressure at 80°C yields $\text{Os}_3(\text{CO})_8(\mu\text{-dppm})(\mu\text{-H})_2$ (**4**) and $\text{Os}_3(\text{CO})_{10}(\mu\text{-dppm})$ (**5**).

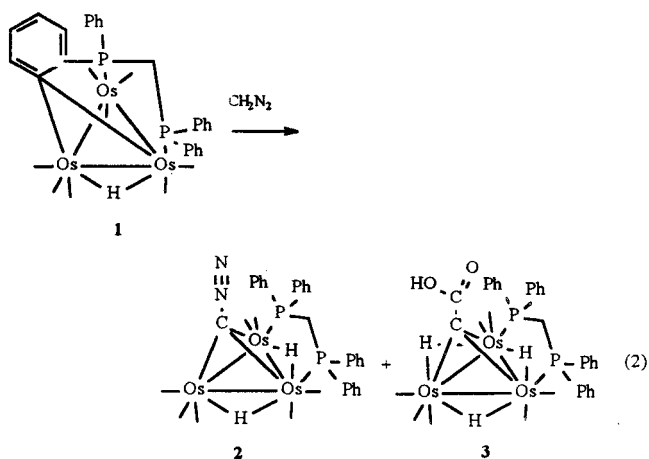
Introduction

The carboxylation of μ_3 -methylidyne and μ_4 -carbido ligands by reaction with nucleophiles is well-known.^{1–5} In the case of the cobalt methylidyne carboxy complexes, these species have proven to be useful for building up mixed metal cluster frameworks.⁶ In the course of our studies of the reactivity of electron-deficient triosmium clusters, we have studied their reactivity with diazomethane. In the case of the electron-deficient quinoline systems $\text{Os}_3(\text{CO})_9(\mu_3\text{-}\eta^2\text{-C}_6\text{H}_9\text{N})(\mu\text{-H})$ insertion by the methylene group into the C(8)–Os bond with accompanying C–H oxidative addition is observed (eq 1).⁷



In the case of the electron-deficient triosmium cluster $\text{Os}_3(\text{CO})_8(\mu_3\text{-}\eta^3\text{-Ph}_2\text{PCH}_2\text{P}(\text{C}_6\text{H}_4)\text{Ph})(\mu\text{-H})$, the reaction with diazomethane takes a completely different course.⁸ Initially, a μ_3 -diazomethylidyne complex, $\text{Os}_3(\text{CO})_7(\mu_3\text{-CN}_2)(\mu\text{-dppm})(\mu\text{-H})_2$ (**2**), forms which subsequently con-

verts to a μ_3 -carboxy methylidyne complex, $\text{Os}_3(\text{CO})_7(\mu\text{-dppm})(\mu_3\text{-CCO}_2\text{H})(\mu\text{-H})_3$ (**3**) in solution (eq 2).



We report here the syntheses and structures of **2** and **3** along with preliminary studies of the mechanism of this interesting interconversion.

Organic diazo compounds are highly reactive substrates having several reaction centers in one molecule and can adopt different coordination modes acting as π - and/or σ -bound terminal, bridging or chelating ligands

[†] Janangirnagar University.

[‡] California State University.

[§] University of Wales Cardiff.

[‡] The University of Montana.

(1) Seyferth, D.; Williams, G. H.; Nivert, C. L. *Inorg. Chem.* **1977**, *16*, 758.

(2) Harris, S.; Bradley, J. S. *Organometallics* **1984**, *3*, 1086 and references therein.

(3) Krause, J.; Jan, D.-Y.; Shore, S. G. *J. Am. Chem. Soc.* **1987**, *109*, 4416.

(4) Holmgren, J. S.; Shapley, J. R. *Organometallics* **1984**, *3*, 1322.

(5) Vollhardt, P. C.; Wolfruber, M. *Angew. Chem.* **1986**, *98*, 919.

(6) Felhner, T. P.; Cen, W. *Inorg. Synth.* **1997**, *31*, 228.

(7) Rosenberg, E.; Kabir, S. E. Manuscript in preparation.

(8) (a) Clucas, J. A.; Harding, M. M.; Smith, A. K. *J. Chem. Soc., Chem. Commun.* **1984**, 949. (b) Clucas, J. A.; Harding, M. M.; Smith, A. K. *J. Chem. Soc., Chem. Commun.* **1985**, 1280. (c) Clucas, J. A.; Harding, M. M.; Smith, A. K. *J. Chem. Soc., Chem. Commun.* **1987**, 1829. (d) Brown, M. P.; Dolby, P. A.; Harding, M. M.; Mathews, A. J.; Smith, A. K.; Osella, D.; Arbrun, D. M.; Gobetto, R. P.; Raithby, R. and Zanello, P. *J. Chem. Soc., Dalton Trans.* **1993**, 827. (e) Brown, M.; Dolby, P. A.; Harding, M. M.; Mathews, A. J.; Smith, A. K. *J. Chem. Soc., Dalton Trans.* **1993**, 1671. (f) Bartlett, R. A.; Cardin, C. D.; Cardin, D. J.; Lawless, G. A.; Power, J. M.; Power, P. P. *J. Chem. Soc., Chem. Commun.* **1988**, 312. (g) Harding, M. M.; Kariuki, B. A.; Mathews, J.; Smith, A. K.; Braunstein, P. *J. Chem. Soc., Dalton Trans.* **1994**, 23. (h) Azam, K. A.; Hursthouse, M. B.; Islam, M. R.; Kabir, S. E.; Malik, K. M. A.; Miah, M. H.; Sudbrake, R. C.; Vahrenkamp, H. *J. Chem. Soc., Dalton Trans.* **1998**, 1097.

to form mono- or multimetallic complexes.⁹ Photochemical or thermal decomposition of diazoalkane provides one of the most general ways for generating carbene intermediates which have drawn much attention because of their important role in Fischer–Tropsch synthesis.¹⁰ Furthermore, with retention of the C–N bond, diazoalkanes can exhibit C- or N-terminal coordination, C=N or N=N side on coordination mode, or can even undergo cycloaddition reactions that constitute useful methods for the synthesis of heterocyclic compounds.¹¹ With trimetallic complexes of osmium, ruthenium, and iron, diazoalkanes have been shown to give both addition and insertion products.¹² The reactions of the unsaturated triosmium cluster $\text{Os}_3(\text{CO})_8\{\mu\text{-P}(\text{Ph})\text{C}_6\text{H}_4\}(\mu\text{-H})$ (**1**) with CO, H_2 , phosphines, phosphites, $[\text{Au}(\text{PPh}_3)]\text{PF}_6$, HBF_4 , and $\text{Sn}[\text{CH}(\text{SiMe}_3)_2]_2$ that give many interesting and potentially useful compounds have also been extensively investigated.⁸ The coordination mode reported here for the diazomethane moiety observed in **2** has not been previously reported.

Results and Discussion

Addition of excess ethereal diazomethane to a dichloromethane solution of the unsaturated compound $\text{Os}_3(\text{CO})_8(\mu\text{-P}(\text{Ph})\text{C}_6\text{H}_4)(\mu\text{-H})$ (**1**) at -10 to 25°C affords two new compounds $\text{Os}_3(\text{CO})_7(\mu_3\text{-CN}_2)(\mu\text{-dppm})(\mu\text{-H})_2$ (**2**) and $\text{Os}_3(\text{CO})_7(\mu_3\text{-CCO}_2\text{H})(\mu\text{-dppm})(\mu\text{-H})_3$ (**3**) in 40 and 25% yield, respectively (eq 2). The molecular structure of **2** is shown in Figure 1, crystal data are in Table 1, and selected distances and bond angles are given in Table 2. The structure consists of an Os_3 triangle with two elongated but almost equal metal–metal bonds ($\text{Os}(1)\text{--}\text{Os}(3) = 2.891(1)$ and $\text{Os}(2)\text{--}\text{Os}(3) = 2.884(1)$ Å) and one significantly shorter metal–metal bond ($\text{Os}(1)\text{--}\text{Os}(2) = 2.751(1)$ Å). The hydride ligands were crystallographically located but not refined and found to bridge the $\text{Os}(1)\text{--}\text{Os}(3)$ and $\text{Os}(2)\text{--}\text{Os}(3)$ edges and this is consistent with elongated Os–Os distances along these edges. The $\text{Os}(2)\text{--}\text{Os}(3)$ edge is also bridged by the dppm ligand. An intriguing structural feature of **2** is the presence of a capping CNN ligand which has been formed by the oxidative addition of C–H bonds of CH_2N_2 . The $\mu_3\text{-CNN}$ moiety symmetrically bridges the three osmium atoms with three equal osmium–carbon bonds ($2.15(1)$ Å). The $\mu_3\text{-CNN}$ ligand is linear within experimental error ($\text{C}(8)\text{--}\text{N}(1)\text{--}\text{N}(2) = 177(2)^\circ$) and lies over the triosmium plane. This is analogous to the

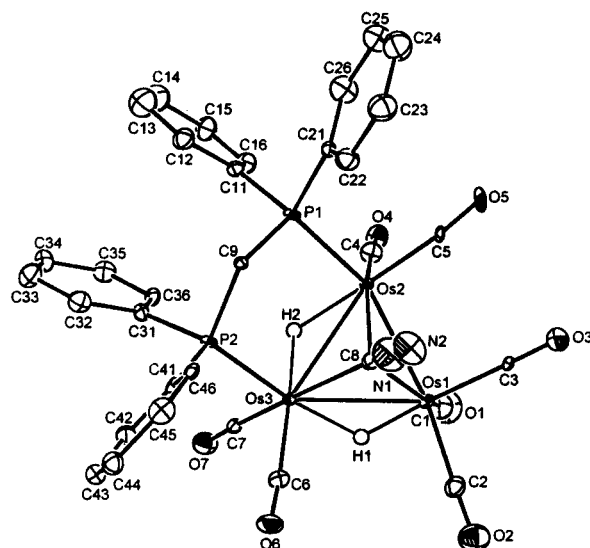


Figure 1. Solid-state structure of $\text{Os}_3(\text{CO})_7(\mu_3\text{-CNN})(\mu\text{-dppm})(\mu\text{-H})_2$ (**2**).

situation observed for $\text{Os}_3(\text{CO})_{10}(\mu_3\text{-CH})(\mu\text{-H})$,¹³ $\text{Os}_3(\text{CO})_{10}(\mu_3\text{-CPh})(\mu\text{-H})$,¹⁴ and $\text{Os}_3(\text{CO})_{10}(\mu_3\text{-CCHMe}_2)(\mu\text{-H})$.¹⁵ This is the first structurally characterized example of a $\mu_3\text{-CNN}$ ligand C-bonded to a metal. The $\text{N}(1)\text{--}\text{N}(2)$ bond distance at $1.14(2)$ Å indicates multiple bonding interaction between two nitrogen atoms while the $\text{C}(8)\text{--}\text{N}(1)$ distance at $1.31(2)$ Å is intermediate between C–N single and double bonds. Another interesting feature of the structure is that the $\text{C}(8)\text{--}\text{N}(1)$ bond vector is nearly perpendicular to the Os_3 plane but is tilted slightly toward $\text{Os}(1)$ ($\text{Os}(1)\text{--}\text{C}(8)\text{--}\text{N}(1) = 126.1(1)^\circ$, $\text{Os}(2)\text{--}\text{C}(8)\text{--}\text{N}(1) = 125.1(1)^\circ$, $\text{Os}(3)\text{--}\text{C}(8)\text{--}\text{N}(1) = 137.1(1)^\circ$). These bond angles are very similar to the corresponding bond angles in $\text{Os}_3(\text{CO})_9(\mu_3\text{-CCO})(\mu\text{-H})_2$.¹⁶ The Os–P bond distances ($\text{Os}(2)\text{--}\text{P}(1) = 2.324(4)$ Å and $\text{Os}(3)\text{--}\text{P}(2) = 2.337(4)$ Å) in **2** are comparable with the values $2.320(3)$ and $2.332(3)$ Å in $\text{Os}_3(\text{CO})_{10}(\mu\text{-dppm})$.¹⁷ The low-temperature (-50°C) ^1H and $^{31}\text{P}\{^1\text{H}\}$ NMR spectroscopic data for **2** are consistent with the solid-state structure. At ambient temperature, however, one observes the onset of an exchange process which averages the two phosphorus environments and can be explained by edge hopping of one of the hydride that bridges the $\text{Os}(1)\text{--}\text{Os}(3)$ edge in the solid-state structure (Figure 2, Scheme 1).

The solid-state structure of **3** is shown in Figure 3, crystal data are given in Table 1, and selected distances and bond angles are in Table 3. The structure is based on a triangular osmium core with two almost equal and one slightly shorter metal–metal bond ($\text{Os}(1)\text{--}\text{Os}(3) = 1.884(2)$, $\text{Os}(2)\text{--}\text{Os}(3) = 2.881(2)$ and $\text{Os}(1)\text{--}\text{Os}(2) = 2.869(1)$ Å). An especially interesting structural feature of **3** is the disposition of the capping CCO_2H ligand. In contrast to $\text{Os}_3(\text{CO})_9(\mu_3\text{-CCO}_2\text{H})(\mu\text{-H})_3$ in which the $\mu_3\text{-CCO}_2\text{H}$ ligand is asymmetrically bonded, the $\mu_3\text{-CCO}_2\text{H}$

(9) (a) Mizobe, Y.; Yshii, Y.; Hidai, M. *Coord. Chem. Rev.* **1995**, *139*, 281 and references therein. (b) Lemenovskii, D. A.; Putala, G. I. M.; Nikonov, N. B.; Kazennova, D. S.; Struchkov, Yu. T. *J. Organomet. Chem.* **1993**, *454*, 123.

(10) (a) Bradley, R. C., III; Pettit, R. J. *J. Am. Chem. Soc.* **1980**, *102*, 6181. (b) Bradley, R. C., III; Pettit, R. J. *J. Am. Chem. Soc.* **1981**, *103*, 1287.

(11) Curtis, M. D.; Messerle, L.; E'Errlco, J. J.; Butler, W. M.; Hay, M. S. *Organometallics* **1986**, *5*, 2283.

(12) (a) Deeming, A. J. *Adv. Organomet. Chem.* **1986**, *26*, 1 and references therein. (b) Smith, A. K. *Comprehensive Organomet. Chem.* **1996**, *7*, 747 and references therein. (c) Holmgren, J. S.; Shapley, J. R. *Organometallics* **1985**, *4*, 793. (d) Holmgren, J. S.; Shapley, J. R.; Wilson, S. R.; Pennington, W. T. *J. Am. Chem. Soc.* **1986**, *108*, 508. (e) Calvert, R. B.; Shapley, J. R. *J. Am. Chem. Soc.* **1977**, *99*, 5225. (f) Freeman, D. W. M.; Hardcastle, K. I.; Isomaki, M.; Kabir, S. E.; McPhillips, T.; Rosenberg, E.; Scott, L. G.; Wolf, E. *Organometallics* **1992**, *11*, 3376. (g) Clauss, A. D.; Shapley, J. R.; Wilson, S. R. *J. Am. Chem. Soc.* **1981**, *103*, 7387. (h) Nucciarone, D.; Taylor, N. J.; Carty, A. J. *Organometallics* **1987**, *3*, 177.

(13) Shapley, J. R.; Cree-Uchiyama, M. E. *J. Am. Chem. Soc.* **1983**, *105*, 140.

(14) Yeh, W. Y.; Shapley, J. R.; Li, Y.; Churchill, M. R. *Organometallics* **1985**, *4*, 767.

(15) Green, M.; Orpen, A. G.; Schaverien, J. C. *J. Chem. Soc., Chem. Commun.* **1984**, 37.

(16) Strickland, D. S.; St. George, G. M.; Shapley, J. R.; Churchill, M. R.; Bueno, C. *Organometallics* **1983**, *2*, 185.

(17) Azam, K. A.; Kabir, S. E.; Malik, K. M. A.; Motallib, M. A. *J. Chem. Crystallogr.* **1999**, *29*, 813.

Table 1. Crystal Data for Compounds **2** and **3**

compound	2	3
empirical form	C ₃₃ H ₂₄ N ₂ O ₇ Os ₃ P ₂ , CH ₂ Cl ₂	C ₃₄ H ₂₆ O ₉ Os ₃ P ₂ , 1/3 C ₆ H ₁₄
form wt	1278.01	1238.13
<i>T</i> (K)	150(2)	293(2)
λ (Å)	0.71073	0.71073
cryst syst	triclinic	monoclinic
space group	<i>P</i> 1	<i>P</i> 2 ₁ / <i>n</i>
unit cell dimens	<i>a</i> = 12.006(4) Å; α = 94.19(2)° <i>b</i> = 12.198(3) Å; β = 92.470(13)° <i>c</i> = 19.460(8) Å; γ = 100.85(2)°	<i>a</i> = 15.383(7) Å; α = 90° <i>b</i> = 12.633(5) Å; β = 90.71(4)° <i>c</i> = 19.460(8) Å; γ = 90°
<i>V</i> , Z	1848.8(9) Å ³ , 2	3781.4(28) Å ³ , 4
<i>d</i> _{calcd} (Mg/m ³)	2.296	2.175
abs coeff (mm ⁻¹)	10.565	10.191
<i>F</i> (000)	1184	2300
cryst size (mm)	0.05 × 0.05 × 0.05	0.20 × 0.15 × 0.14
θ range for data collection (deg)	2.18 to 25.07	1.68 to 21.00
index ranges	14 ≤ <i>h</i> ≤ 11, −11 ≤ <i>k</i> ≤ 14, −13 ≤ <i>l</i> ≤ 15	−15 ≤ <i>h</i> ≤ 15, 0 ≤ <i>k</i> ≤ 12, −0 ≤ <i>l</i> ≤ 19
reflns coll	7375	7845
ind reflns	4847 { <i>R</i> _(int) = 0.0456}	4047 { <i>R</i> _(int) = 0.0711}
abs corr	DIFABS (Walker and Stuart, 1983)	Psi scans
max and min transmission	0.998 and 0.865	0.3504 and 0.1986
refinement method	full-matrix least-squares on <i>F</i> ²	full-matrix least-squares on <i>F</i> ²
data/restraints/params	4847/0/403	4047/0/454
GOF on <i>F</i> ²	0.934	1.002
final <i>R</i> indices [<i>I</i> > 2 σ (<i>I</i>)]	<i>R</i> ₁ = 0.0365, <i>wR</i> ₂ = 0.0889	<i>R</i> ₁ = 0.0917, <i>wR</i> ₂ = 0.0779
<i>R</i> indices (all data)	<i>R</i> ₁ = 0.0484, <i>wR</i> ₂ = 0.0905	<i>R</i> ₁ = 0.0917, <i>wR</i> ₂ = 0.0896
largest diff. peak and hole	1.170 and −1.573 e Å ⁻³	1.214 and −0.631 e Å ⁻³

Table 2. Selected Distances (Å) and Angles(deg) for **2**

Distances			
Os(1)–Os(2) ^a	2.742(1)	C(8)–N(1)	1.31(2)
Os(1)–Os(3)	2.893(1)	N(1)–N(2)	1.14(2)
Os(2)–Os(3)	2.883(1)	P(1)–C(9)	1.85(1)
Os(1)–C(8)	2.15(1)	P(2)–C(9)	1.82(1)
Os(2)–C(8)	2.15(1)	P(1)–C(11)	1.821(8)
Os(3)–C(8)	2.15(1)	P(1)–C(21)	1.840(7)
Os(2)–P(1)	2.324(4)	P(2)–C(31)	1.813(7)
Os(3)–P(2)	2.337(4)	P(2)–C(41)	1.814(6)
Angles			
Os(1)–Os(2)–Os(3)	61.85(3)	C(8)–N(1)–N(2)	177(2)
Os(1)–Os(3)–Os(2)	56.67(3)	P(1)–C(9)–P(2)	115.9(6)
Os(2)–Os(1)–Os(3)	61.47(3)	Os(1)–C(8)–N(1)	126.(1)
Os(2)–Os(1)–C(8)	50.5(4)	Os(2)–C(8)–N(1)	125.(1)
Os(3)–Os(1)–C(8)	47.7(4)	Os(3)–C(8)–N(1)	137.(1)
Os(3)–Os(2)–P(1)	93.84(9)	P(1)–Os(2)–C(8)	98.7(3)
Os(2)–Os(3)–P(2)	91.82(9)	P(2)–Os(3)–C(8)	95.4(4)
Os–C–O ^b	176.(1)		

^a Numbers in parentheses are average standard deviations.^b Average values.

ligand in **3** is symmetrically capped with Os(1)–C(1) = 2.07(2), Os(2)–C(1) = 2.06(2) and Os(3)–C(1) = 2.06(2) Å. The Os–C bond distances are on the average 0.04 Å shorter than the corresponding bonds in Os₃(CO)₉(μ_3 -CCO₂H)(μ -H)₃.³ The C(1)–C(2) bond vector is nearly perpendicular to the Os₃ plane but is tilted slightly toward Os(1)(Os(1)–C(1)–C(2) = 125.(1) Å, Os(2)–C(1)–C(2) = 125.(1) Å, Os(3)–C(1)–C(2) = 127.(1) Å). These bond angles are similar to the corresponding bond angles in (μ -H)₃Os₃(CO)₉(μ_3 -CCOOH).³ The dppm ligand bridges the Os(3)–Os(1) edge, and the P–Os bond distances are Os(3)–P(2) = 2.308(5) and Os(1)–P(1) = 2.342(5) Å. Within the CCO₂H unit the C(1)–C(2), C(2)–O(1), and C(2)–O(2) bond distances of 1.49(2), 1.24(2), and 1.31(2) Å and the C(1)–C(2)–O(1), C(1)–C(2)–O(2), and O(1)–C(2)–O(2) angles of 125(2), 116(1), and 118(2) Å are comparable with those of the corresponding distances and angles in Os₃(CO)₉(μ_3 -CCO₂H)(μ -H)₃.^{3,4} The C(1)–C(2) bond distance of the CCO₂H unit in **3** is 1.50(3) Å and is similar to the distances in benzoic and

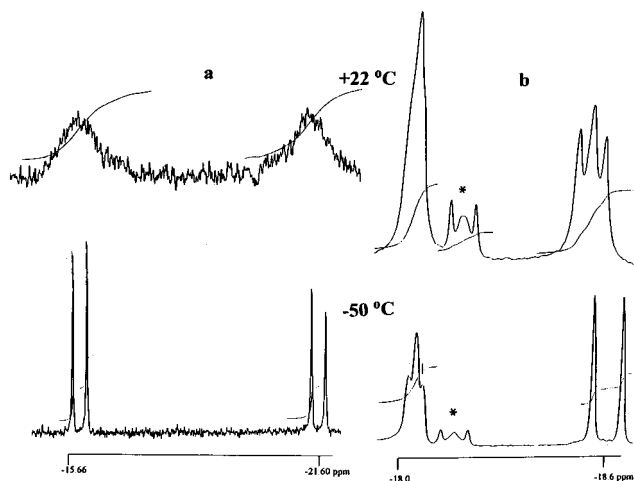
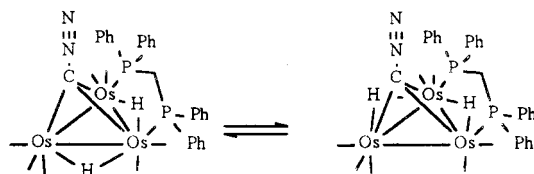


Figure 2. Variable-temperature ³¹P (a) and ¹H (b) NMR of Os₃(CO)₇(μ_3 -CNN)(μ -dppm)(μ -H)₂ (**2**) at 162 and 400 MHz, respectively (peak marked with an asterisk is due to the presence of a small amount of **3**).

Scheme 1



acetic acids which are 1.48(2) and 1.54(2) Å, respectively. A key feature of the structure of **3** is that the Os–C–Os bond angles Os(1)–C(1)–Os(2) = 88.9(7), Os(2)–C(1)–Os(3) = 89.7(7), and Os(3)–C(1)–Os(1) = 89.6(6) Å are close to right angles. To our knowledge, compound **3** represents the second reported structure of a triosmium compound containing μ_3 -CCO₂H ligand and is the dppm substituted analogue of the first reported compound Os₃(CO)₉(μ_3 -CCO₂H)(μ -H)₃, which was synthesized from the reaction of Os₃(CO)₉(μ_3 -CCO)-(μ -H)₂ with an H₂O–HCl mixture.³ The analogous

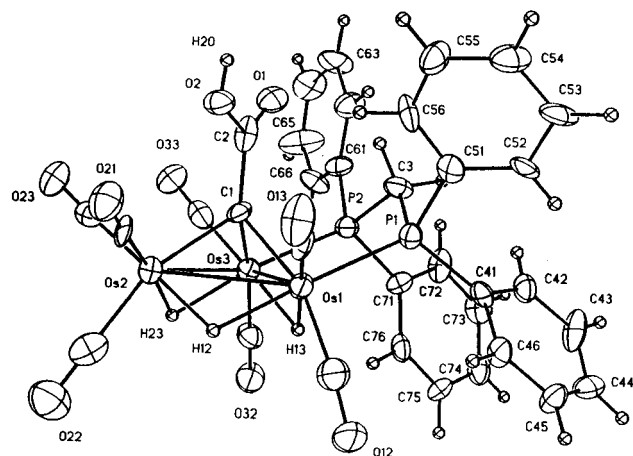


Figure 3. The solid-state structure of $\text{Os}_3(\text{CO})_7(\mu_3\text{-CCO}_2\text{H})(\mu\text{-dppm})(\mu\text{-H})_3$ (**3**) showing the calculated positions of the hydride ligand.

Table 3. Selected Distances (Å) and Bond Angles (deg) for **3**

Distances			
Os(1)–Os(2) ^a	2.869(1)	C(1)–C(2)	1.49(2)
Os(1)–Os(3)	2.884(1)	C(2)–O(2)	1.31(1)
Os(2)–Os(3)	2.881(1)	C(2)–O(1)	1.24(2)
Os(1)–C(1)	2.07(1)	P(1)–C(3)	1.87(1)
Os(2)–C(1)	2.06(1)	P(2)–C(3)	1.81(1)
Os(3)–C(1)	2.06(1)	P(1)–C(41)	1.81(1)
Os(1)–P(1)	2.342(5)	P(1)–C(51)	1.82(1)
Os(3)–P(2)	2.308(5)	P(2)–C(61)	1.82(1)
Os–CO ^b	1.84(2)	P(2)–C(71)	1.82(1)
Angles			
Os(1)–Os(2)–Os(3)	60.22(4)	C(1)–C(2)–O(1)	125.1(1)
Os(1)–O(3)–Os(2)	59.68(4)	C(1)–C(2)–O(2)	116.1(1)
Os(2)–Os(1)–Os(3)	60.10(4)	O(1)–C(2)–O(2)	118.2(2)
Os(3)–Os(1)–C(1)	45.5(5)	Os(1)–C(1)–C(2)	125.1(1)
Os(2)–Os(3)–C(1)	45.5(5)	Os(2)–C(1)–C(2)	125.1(1)
Os(1)–Os(3)–C(1)	45.7(4)	Os(3)–C(1)–C(2)	127.1(1)
Os(1)–Os(2)–C(1)	46.04(4)	Os(1)–C(1)–Os(2)	88.2(6)
Os(3)–Os(2)–C(1)	45.7(4)	Os(1)–C(1)–Os(3)	88.7(6)
Os(3)–Os(1)–P(1)	93.3(1)	Os(2)–C(1)–Os(3)	88.8(7)
Os(1)–Os(3)–P(2)	91.1(1)	P(1)–C(3)–P(2)	114.9(8)
Os–CO ^b	176.2(2)		

^a Numbers in parentheses are average standard deviations.

^b Average values.

complexes $\text{Ru}_3(\text{CO})_9(\mu_3\text{-CCO}_2\text{H})(\mu\text{-H})_3$ ⁴ and $\text{Cp}_3\text{Co}_3(\mu_3\text{-CH})(\mu_3\text{-CCO}_2\text{H})$ ⁵ have also been reported based on spectroscopic data. The spectroscopic data of **3** are in accord with the solid-state structure. The compound $\text{Os}_3(\text{CO})_7(\mu_3\text{-CNN})(\mu\text{-dppm})(\mu\text{-H})_2$ (**2**) is a logical precursor to **3** by the reaction of **2** with CO and H₂O. Solutions of **2** slowly and partially convert to **3** and are accompanied decomposition of **2**. The reaction of **2** with 1 atm of CO and H₂O in an NMR tube results in the quantitative and instantaneous conversion of **2** to **3**. The formation of **3** from the reaction **2** with CO and H₂O most probably proceeds via the intermediacy of the ketenylidene compound $\text{Os}_3(\text{CO})_7(\mu_3\text{-CCO})(\mu\text{-dppm})(\mu\text{-H})_2$ (Scheme 2). When ¹³CO is used to promote the transformation of **2** to **3**, we do not observe selective incorporation of the label into the carboxylic acid. Instead, we observe equal distribution into all seven carbonyl resonances of **3**. This result suggests that CO migrates from the metal core to form the proposed μ_3 -ketenylidene intermediate which reacts rapidly with H₂O to form **3**. This type of reaction pathway has also been demonstrated for the formation of μ_3 - and μ_4 -methylidyne carboxylates in the

case of Fe₄ and Co₃ cluster systems.^{1,2} The source of CO in the absence of added CO is probably from minor nonspecific decomposition of **2**. That **2** converts to **3** rapidly with CO and water while $\text{Os}_3(\text{CO})_9(\mu_3\text{-CCO})(\mu\text{-H})_2$ requires strong acid suggests that the electron-donating dppm further polarizes the proposed ketenylidene intermediate (by increasing back-donation from the metal to the ketenylidene ligand) making it more subject to nucleophilic attack (more C=C=O[−] character) by trace moisture. This also explains why we were unable to observe the ketenylidene.

To examine the reactivity of the coordinated μ_3 -CNN group, we investigated the reaction of **2** with molecular hydrogen. The objective was to see if N₂ loss from the μ_3 -CNN ligand followed by H₂ oxidative addition would result in the formation of the methylidyne compound $\text{Os}_3(\text{CO})_7(\mu\text{-CH})_7(\mu\text{-dppm})(\mu\text{-H})_2$. However, treatment of **2** with molecular hydrogen at atmospheric pressure at 80 °C gives the previously reported clusters $\text{Os}_3(\text{CO})_8(\mu\text{-dppm})(\mu\text{-H})_2$ (**5**)^{8b} and $\text{Os}_3(\text{CO})_{10}(\mu\text{-dppm})$ (**4**)^{8a} in 65 and 20% yields, respectively²⁰ instead of the desired methylidyne compound. Here again, the presence of the dppm ligand apparently polarizes the osmium carbon bonds so that reductive elimination of methane is favored over oxidative addition of hydrogen to the cluster. Additionally, it seems likely that **2** converts to **3** during hydrogenolysis and that the organic coproduct is acetic acid (Scheme 2). Further studies on the reactivity of **2** are in progress.

Experimental Section

Reactions were performed in an atmosphere of nitrogen and worked up in the air. Solvents were distilled from the appropriate drying agents directly before use. ¹H, ³¹P, and ¹³C NMR were obtained on a Varian 400 MHz Unity Plus spectrometer and IR data was obtained on a Shimadzu FT-IR. Elemental analyses were performed by Schwarzkopf Microanalytical Labs, Woodside, New York.

Reaction of 1 with Diazomethane. To a CH₂Cl₂ solution (5 mL) of **1** (0.080 g, 0.068 mmol) was added a freshly prepared ethereal solution of diazomethane (~0.700 g, ~16.6 mmol) at −10 °C, and the reaction mixture was stirred for 1 h. The solvent was removed under reduced pressure, and the residue was chromatographed by TLC on silica gel. Elution with hexane/CH₂Cl₂ (9:1, v/v) gave $\text{Os}_3(\text{CO})_7(\mu_3\text{-CN}_2)(\mu\text{-dppm})(\mu\text{-H})_2$ (**2**) (0.032 g, 40%) and $\text{Os}_3(\text{CO})_7(\mu_3\text{-CCO}_2\text{H})(\mu\text{-dppm})(\mu\text{-H})_3$ (**3**) (0.020 g, 25%) as yellow crystals from hexane/CH₂Cl₂ at −20 °C.

Analytical and Spectroscopic Data for 2. Anal. Calcd for C₃₃H₂₄N₂O₇Os₃P₂: C, 33.22; H, 2.03; N, 2.35. Found: C, 33.35; H, 2.12; N, 2.49. IR (ν_{CO}, CH₂Cl₂): 2070s, 2033vs, 1993m, 1975m, 1929w cm^{−1}. ¹H NMR (400 MHz, CDCl₃, −50 °C): δ 7.21 (m, 20H), 4.60 (AB, 1H, *J*(composite) = 10.8 Hz), 3.38 (AB, 1H, *J*(composite) = 12.0 Hz), −18.06 (t, 1H, *J* = 8.4 Hz), −18.64 (d, 1H, *J* = 34.8 Hz). ³¹P{¹H}NMR (CDCl₃): δ −15.7 (d), −21.7 (d, *J* = 54.0 Hz).

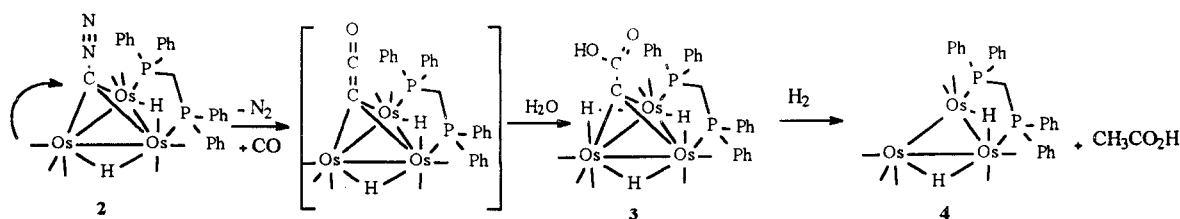
Analytical and Spectroscopic Data for 3. Anal. Calcd for C₃₄H₂₆O₉Os₃P₂: C, 33.71; H, 2.17. Found: C, 33.92; H, 2.28. IR (ν_{CO}, CH₂Cl₂): 2087s, 2024vs, 1998m, 1958s cm^{−1}. ¹H NMR (400 MHz, CDCl₃): δ 10.0 (br. 1H), 7.34 (m, 20H), 4.86 (AB, 1H, *J*(composite) = 13.8 Hz), 4.35 (AB, 1H, *J*(composite) = 11.2 Hz), −18.18 (virtual triplet, 2H, *J*(composite) = 16.2 Hz), −19.23(t, 1H, *J* = 9.8 Hz). ³¹P{¹H}NMR (CDCl₃): δ −13.4(s).

(18) Darr, J. A.; Drake, S. R.; Hursthouse, M. D.; Malik, K. M. A. *Inorg. Chem.* **1993**, 32, 5704.

(19) Walker, N. P. C.; Stuart, D. *Acta Crystallogr.* **1983**, A39, 158.

(20) Sheldrick, G. M. SHELXS-86 *Acta Crystallogr.* **1990**, A46, 467.

Scheme 2



Reaction of **2 with CO and H₂O.** CO gas was bubbled through a CDCl₃ (0.5 mL) solution of **2** (0.035 g, 0.029 mmol) containing 4 μ L of H₂O in an NMR tube. The ¹H and ³¹P{¹H} NMR spectra indicated complete conversion to Os₃(CO)₇(μ_3 -CCO₂H)(μ -dppm)(μ -H)₃. Work up and chromatographic separation as mentioned before gave **3** (0.033 g, 92%).

Reaction of **2 with H₂.** Hydrogen gas was bubbled through a refluxing cyclohexane solution (30 mL) of **2** (0.075 g, 0.062 mmol) for 4 h. The solvent was removed under reduced pressure and the residue was chromatographed by TLC on silica gel. Elution with hexane/CH₂Cl₂ (4:1, v/v) developed two bands which afforded Os₃(CO)₁₀(μ -dppm)(**5**) (0.015 g, 20%) and Os₃(CO)₈(μ -dppm)(μ -H)₂ (**4**) (0.047 g, 65%).

X-ray Structure Determination of **2.** Crystallographic measurements for compound **2** were made at 150 K using graphite monochromatic Mo K α radiation (λ = 0.71073 Å) on an Enraf Nonius FAST area detector diffractometer by following procedures described earlier.¹⁸ The data were corrected for absorption effects by using the DIFABS method.¹⁹ The structure was solved by direct methods²⁰ and refined²¹ on F^2 using all unique data with intensities >0. The two bridging hydrides were located from the difference map, but not refined. All other hydrogen atoms were included in calculated positions (riding model). All non-hydrogen atoms were refined anisotropically. The phenyl rings were treated as idealized hexagons with C–C = 1.390 Å and C–C–C (internal) angles = 120.0°. The structure refined to a final R_1 [on F , 3865 data with $F^2 > 2\sigma(F^2)$] = 0.0365 and wR_2 [on F^2 , all 4847 data] = 0.0905. The crystal data and refinement details are given in Table 1.

X-ray Structure Determination of **3.** Crystals of **3** for X-ray examination were obtained from a saturated solution of hexane/dichloromethane solvents at –20 °C. A suitable crystal was mounted on a glass fiber, placed in a goniometer head on an Enraf Nonius CAD4 diffractometer, and centered optically. Unit cell parameters and an orientation matrix for data collection were obtained by using the centering program in the CAD4 system. Details of the crystallographic data are given in Table 1. The actual scan range was calculated by scan width = scan range + 0.35 tan θ , and backgrounds were measured by using the moving-crystal-moving-counter technique at the beginning and end of each scan. Two representative reflections were monitored every 2 h as a check on instrument and crystal stability. Lorentz, polarization, and decay corrections were applied to the raw crystal data, as was

an empirical absorption correction based on a series of Ψ scans. The weighting scheme used during refinement was $1/\sigma^2$, based on counting statistics.

The structure was solved by Direct methods using SHELXTL/PC²¹ which revealed the positions of most of the atoms. Remaining non-hydrogen atoms were found by successive refinement and ΔF syntheses. Hydrogen atoms were placed in their expected chemical positions by using the HFIX command and were included as riding atoms. The positions of the bridging hydride atoms were calculated by using HYDEX.²² All non-hydrogen atoms were refined anisotropically. All data processing, structure solution, refinement and preparation of figures and tables for publication were carried out on PC's using SHELXTL/PC. Neutral atom scattering factors and values of $\Delta f'$ and $\Delta f''$ were from Volume C of the International Tables for Crystallography.²³

The final difference Fourier indicated the presence of some solvent in the lattice, which was modeled, although not well, as a disordered hexane molecule with an occupancy factor of about 0.3. There is a strong intermolecular hydrogen bond between the carboxyl groups on neighboring molecules. The O(H)–O distance is 2.67 Å which is about the same as that observed in benzoic acid dimers.²⁴

Acknowledgment. Support of this work by the Ministry of Science and Technology, the Peoples Republic of Bangladesh, is gratefully acknowledged. Edward Rosenberg thanks the National Science Foundation (CHE 9625367) for support. We are also thankful to Professor M. B. Hursthouse (Southampton) for access to the EPSRC-supported X-ray data collection facilities.

Supporting Information Available: Tables giving X-ray crystallographic data for **2** and **3**. This material is available free of charge via the Internet at <http://pubs.acs.org>.

OM000322B

(22) Orpen, A. G. *J. Chem. Soc., Dalton Trans.* **1980**, 2509.

(23) *International Tables for X-ray Crystallography*; Kluwer Academic Publishers: Dordrecht, 1992; Vol. C, Tables 6.1.1.4, pp 500–502 and 4.2.6.8, pp 219–222.

(24) Crystallographic data for the structural analyses have been deposited with the Cambridge Crystallographic Data Centre, CCDC Nos. 141586 and 141382 for compounds **2** and **3**. Copies of this information may be obtained free of charge from Director, CCDC, 12 Union Road, CB21EZ, UK [fax int.code +44(1223)336033 or e-mail deposit@ccdc.cam.ac.uk or <http://www.ccdc.cam.ac.uk>].

(21) SHELXTL/PC, Siemens Analytical X-ray Instruments, Inc., Madison, WI.